18

Modeling DOM from the ecosystem to global scales

Naomi M. Levine^a and Timothy DeVries^b

^aDepartment of Biological Sciences, University of Southern California, Los Angeles, CA, United States ^bDepartment of Geography and Earth Research Institute, University of California, Santa Barbara, CA, United States

	JUT	LINE	
18.1 Introduction18.2 Modeling carbon and energy flow	803 vs 804	18.4 Data-constrained models of DOC cycling	810
18.2.1 The beginning: Food web models and biogeochemical		18.5 Global distribution, inventories, and production rates of DOC	812
models 18.2.2 Basic formulation of moderr ocean biogeochemical models		18.6 Carbon export and sequestration by DOC	814
18.2.3 Current state of DOM modeling in earth system which was a system of the earth system of the earth system which was a system of the earth system which was a system of the earth system of the earth system which was a system of the earth	dels 808	18.7 Areas for future advancement in DOM modeling	816
18.3 Modeling more complex organic		Acknowledgments	817
matter dynamics	809	References	817

18.1 Introduction

Numerical models provide a tool for synthesizing the impacts of dissolved organic matter (DOM) cycling on large-scale processes such as ecosystem dynamics and carbon cycling and for developing hypotheses that can be further tested experimentally. This chapter outlines ways in which DOM cycling has been incorporated into numerical models, key findings that have been elucidated through DOM modeling efforts, and future promising directions for DOM models.

Here we focus on DOM models aimed at capturing ecosystem- to global-scale dynamics. Specifically, we cover two broad classes of large-scale DOM models: mechanistic biogeochemical models and empirical data-constrained models. Both models provide key, but different, insights into DOM modeling. Biogeochemical models provide insight into mechanisms and can provide predictions as to how the system will respond to perturbations such as shifts in climate. Data-constrained models provide our current best estimates for standing stocks and fluxes in the current ocean.

Another class of models focuses more on the molecular scale and provides critical insight into the chemical diversity of DOM and rates of DOM transformations. For more on these models, we refer the reader to Chapter 13: Reasons Behind the Long-Term Stability of Dissolved Organic Matter by Dittmar and Lennartz. Finally, many of the exciting new advances related to DOM production and consumption (as described in other chapters of this book) have not yet been incorporated into DOM models and so are not covered in this chapter, although we do highlight some key areas for future model development.

18.2 Modeling carbon and energy flows

18.2.1 The beginning: Food web models and biogeochemical models

Numerical models have long been a key ecological tool for integrating observations and theory dating back to the pioneering marine food web models of Riley (Riley, 1946; Riley and Bumpus, 1946; Riley, 1947). These early predator-prey models were focused on the growth of phytoplankton and zooplankton and tracked the flow of material and energy through marine ecosystems. The relatively narrow focus of these early models was expanded following the influential paper of Pomeroy (1974), which argued that our view of marine food webs needed to encompass energy flows through DOM and bacteria (Fig. 18.1A). At the time, it was estimated that microbes accounted for 50%–90% of ecosystem respiration. Thus, Pomeroy argued that, given the large fluxes through these pools, understanding these "unseen strands in the food web" was crucial both for understanding the ecology of the ocean and for better fisheries management.

In the early 1980s, several researchers began incorporating DOM dynamics into planktonic food web models (e.g., Williams, 1981; Pace et al., 1984). For example, the model by Pace et al. (1984) included 14 biotic pools, including a DOM pool, two detritus pools, and free-living and particle-attached bacteria pools. In contrast with previous models, which assumed that all primary production was grazed by zooplankton, the Pace model routed 50% of primary productivity through DOM, implicitly simulating viral and bacterial decomposition of primary production. This model investigated ecological efficiency in different continental shelf environments. Pace and colleagues showed that DOM and POM production and cycling could play a critical role in energy flows and result in variable ecosystem efficiency (defined as the fraction of ingested carbon converted to biomass at each trophic level) from 1% to 73%.

Biogeochemical models trace their roots back to the same food web modeling studies from the 1940s and 1950s (e.g., Riley, 1946). The key divergence between biogeochemical and food web models arose in the late 1970s when biogeochemical models focused more explicitly on resolving nutrient cycling and primary productivity and neglected higher trophic levels.

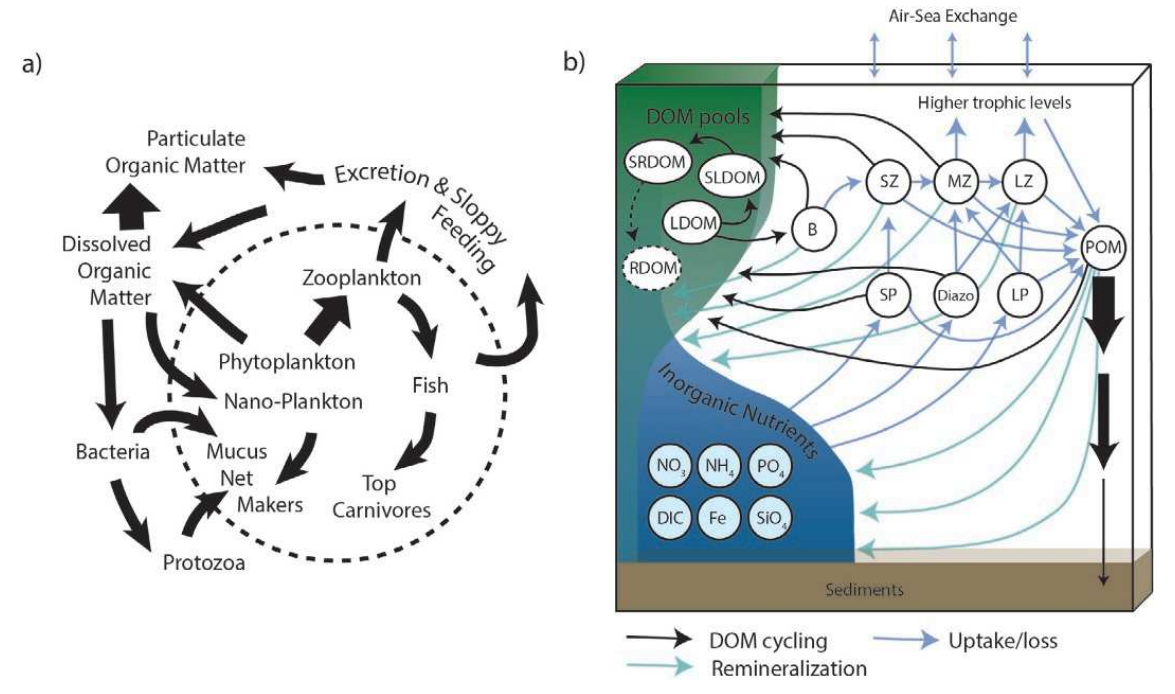


FIG. 18.1 Early ocean food web modeling perspective (A) compared to present-day state-of-the-art biogeochemical models (B). Pomeroy proposed expanding the classic view of the ocean food web (inside the *dashed circle*) to include fluxes of organic matter (A). Biogeochemical models today typically resolve the fluxes of multiple nutrients (e.g., carbon, nitrogen, phosphorus, iron, and silica) and include multiple pools of phytoplankton and zooplankton, such as small phytoplankton (SP), large phytoplankton (LP), diazotrophs (Diazo), small zooplankton (SZ), medium zooplankton (MZ), and large zooplankton (LZ) (B). These models also include dynamic organic matter cycling with multiple organic matter pools, including labile DOM (LDOM), semilabile DOM (SLDOM), semirefractory DOM (SRDOM), and particulate organic matter (POM). Most biogeochemical models do not explicitly resolve refractory DOM (RDOM), but we include it here for completeness. Cycling of DOM is shown with *black arrows*, uptake of inorganic nutrients and consumption/loss/mortality are shown with *blue arrows*, and remineralization is shown with *teal arrows*. (A) *Redrawn from Pomeroy* (1974), Fig. 1. (B) *Redrawn from Stock et al.* (2020), Fig. 1.

These models began to study the underlying mechanisms behind variations in primary productivity, including environmental drivers (e.g., Kiefer and Kremer, 1981) and inorganic nutrient cycling—for example, the difference between primary production driven by nitrate (new production) and ammonium (regenerated production) (Jamart et al., 1977; Vézina and Platt, 1987). At around the same time that ecologists were starting to incorporate DOM cycling into food web models, the chemical oceanographic community began to call for the incorporation of DOM into biogeochemical models to evaluate the role that DOM plays in carbon and nutrient cycling and phytoplankton growth (e.g., Williams et al., 1988).

The seminal study of Fasham et al. (1990) investigated the role of DOM in the cycling of nitrogen through the marine food web. This model included dissolved organic nitrogen (DON) production through phytoplankton exudation, detritus decomposition, and "sloppy feeding" by zooplankton. In turn, DON was consumed by a bacterial pool that released ammonium. The authors concluded that "detrital material behaves like a capacitor, allowing higher regeneration rates and greater production." Around the same time, Najjar et al. (1992) published a phosphorus-based model that included dissolved and particulate pools of organic

phosphorus. This study showed that when dissolved organic pools were omitted from the model, nutrients became trapped in the surface ocean below the euphotic zone resulting in concentrations greater than observations. When these waters were upwelled, this generated greater surface concentrations of phosphorus and higher rates of primary productivity than observations. Including DOP and longer timescales for particle remineralization alleviated the "nutrient trapping" (Najjar et al., 1992) observed in previous models. These studies highlighted the significance of organic matter pools in capturing nutrient concentrations, regenerated production, and the timescales of phytoplankton dynamics. This was a crucial step toward including DOM in biogeochemical models.

The next generation of biogeochemical models, often called Nutrient-Phytoplankton-Zooplankton-Detritus (NPZD) models, was developed in the late 1990s and early 2000s. Similar to Fasham et al. (1990), NPZD models explicitly tracked the flow of carbon and nutrients through broadly defined detrital fractions (e.g., Doney et al., 1996). The NPZD models also began to explicitly represent the cycling of multiple nutrients independently (e.g., Moore et al., 2002). For example, the Biogeochemistry Elemental Cycle (BEC) model incorporated carbon, nitrogen, phosphorus, and iron cycling, and the resulting multiple nutrient limitation on primary productivity into a marine ecosystem model (Moore et al., 2002). The BEC model represented two detritus classes, one sinking and one nonsinking (i.e., DOM plus small POM), and used fixed elemental stoichiometries for the ecosystem components. Nitrogen fixation was also included in this model and was shown to be an important source of DON. This was one of the first models to represent all the organic and inorganic carbon and nutrient pools that are now considered standard in ocean biogeochemical models (Fig. 18.1B).

The first models to include multiple nonliving OM pools differentiated these pools based on size (e.g., sinking vs nonsinking as described before). This differentiation is consistent with operationally defined observations of organic matter concentrations into dissolved and particulate fractions (Benner and Amon, 2015) and remains an important framework for capturing carbon export flux through sinking OM (e.g., Omand et al., 2020). While size remains the primary way in which POM is differentiated from DOM in models and observations, as biogeochemical models have increased in complexity, they have begun to incorporate the cycling of multiple DOM pools. Typically, these different DOM groups are defined along a lability spectrum based on turnover rates from labile DOM (LDOM in Fig. 18.1B) to semilabile (SLDOM) to semirefractory (SRDOM) to refractory (RDOM) (see Chapter 5 for further discussion). These different lability pools and how they are modeled are discussed in greater detail later (Section 18.3). First, we present an overview of the basic formulation of modern ocean biogeochemical models.

18.2.2 Basic formulation of modern ocean biogeochemical models

While each biogeochemical model is slightly different in terms of the processes that are included and the formulation of the dynamics, these models all follow the same basic formulation. Specifically, the models use a set of coupled differential equations to express the production and loss terms of each component of the ecosystem. As described in Section 18.2.1 and illustrated in Fig. 18.1B, these models track some combination of inorganic nutrients

(e.g., nitrate, ammonium, phosphate), one to multiple phytoplankton groups, often a predator of phytoplankton (nominally a zooplankton), and one to multiple detrital pools. Here, we outline the generic equations that are used in these models, including those for DOM cycling. Ocean circulation and mixing play an important role in biogeochemical cycling (e.g., by providing nutrients through upwelling), and so for completeness, we include this term on the left-hand side of the equations (*circulation*), but here we will focus on the biological drivers of changes in the model state variables.

Changes in inorganic nutrients (N) are modeled generally as follows:

$$\frac{dN}{dt} + \text{circulation} = -\sum_{i} \text{uptake} + \sum_{j} \text{production}$$
 (18.1)

where uptake is summed over i phytoplankton groups. There is also production of nutrients by some subset j of the ecosystem, for example the production of ammonium or phosphate through the consumption of organic matter. This last term is thus often linked to the decomposition of DOM. Many models also include external sources and sinks of nutrients from rivers, atmospheric deposition, or sedimentary exchanges (Fig. 18.1B). These sources would be added as additional terms in Eq. (18.1).

Phytoplankton dynamics are represented using some form of the equation:

$$\frac{dP_i}{dt} + \text{circulation} = \mu_i \gamma_i^N \gamma_i^T \gamma_i^L P_i - m_i P_i - \sum_j g_{i,j} P_i Z_j - agg$$
 (18.2)

where the first term on the right-hand side (RHS) defines the gross phytoplankton biomass growth, which is related to the inorganic nutrient uptake rate (first term RHS in Eq. 18.1). Specifically, μ_i is the phytoplankton group-specific growth rate, γ_i^N is the nutrient limitation of phytoplankton group i, γ_i^T is the temperature limitation of group i, and γ_i^L is the light limitation of group i. Phytoplankton loss occurs through a linear density-dependent loss term (second term RHS in Eq. 18.2) and/or through explicit grazing (third term RHS in Eq. 18.2) where $g_{i,j}$ is the grazing rate of zooplankton group j on phytoplankton group j. Many models also include an additional loss term for phytoplankton (agg) which represents the formation of aggregates or particles.

For models that include the excretion of DOM by phytoplankton, this is typically encompassed within the linear, density-dependent mortality term (m_iP_i), which represents all nongrazing biomass loss. Specifically, a fraction of this mortality term is added as a source of DOM (see Eq. 18.4). Sometimes this term is broken out explicitly to represent exudation and viral lysis separately, but even then, these processes are typically represented using the same linear form (e.g., Stock et al., 2014).

Zooplankton dynamics are described by

$$\frac{dZ_j}{dt} + \text{circulation} = \sum_i \gamma_g g_{i,j} P_i Z_j - m_j Z_j - a Z_j^n$$
(18.3)

where the first term represents the ingestion of phytoplankton by zooplankton group j. Only a fraction (γ_g) of ingested prey $(g_{i,j}P_iZ_j)$ is converted to biomass while the remainder $(1-\gamma_g)$ represents the fraction lost to egestion, "sloppy feeding," and respiration. Some of this $(1-\gamma_g)$

fraction is routed to DOM, some to POM, and the rest to inorganic nutrients. Zooplankton loss terms include a linear mortality (m_j) and/or a "quadradic" mortality aZ_j^n (we use the notation n as various models use different exponents, though n = 2 or 1.5 are typical values).

The change in the DOM pool is represented as follows:

$$\frac{dDOM_k}{dt} + \text{circulation} = \sum_{i} f_{ex,k} m_i P_i + \sum_{j} f_{g,k} g_{i,j} P_i Z_j + f_{pom,k} \kappa_{pom} POM - \kappa_k \gamma^* DOM_k$$
 (18.4)

where the first three terms on the RHS represent the three primary DOM sources: (1) direct release from phytoplankton either through exudation or nongrazing mortality, (2) "sloppy feeding" by zooplankton on phytoplankton or zooplankton egestion, and (3) release of DOM as a by-product of POM degradation which proceeds at rate κ_{pom} . Specifically, $f_{ex,k}$ is the fraction of phytoplankton mortality that is routed through DOM (source 1), $f_{g,k}$ is the fraction of grazed phytoplankton biomass that is released to DOM (source 2), and $f_{pom,k}$ is the fraction of POM degradation that is released as DOM (source 3). These models typically assume that the loss rate of DOM follows first-order kinetics, whereby the loss rate is proportional to the concentration of the substrate. The DOM loss rate constant (κ_k) is often scaled by environmental factors (γ^*) such as temperature and/or light. For models that explicitly incorporate bacterial dynamics, κ is a function of bacterial biomass.

Biogeochemical models typically include between one (k=1) and four DOM (k=4) pools where the production terms and degradation rates vary for each group. Models that represent multiple lability classes (e.g., LDOM, SLDOM, SRDOM, and RDOM) often transfer DOM sequentially from the most labile to the most recalcitrant pools (Fig. 18.1B). This formulation is inspired by the concept of the "microbial carbon pump" in which microbial degradation preferentially removes labile dissolved organic carbon (DOC) molecules or transforms DOC molecules to recalcitrant forms that accumulate in the ocean (Jiao et al., 2010). To incorporate this transfer between DOM pools, an additional term(s) similar to POM degradation term would be added to the RHS of Eq. (18.4).

18.2.3 Current state of DOM modeling in earth system models

Since the early 2000s, the biogeochemical models described in Section 18.2.2 have been embedded into state-of-the-art Earth System Models (ESMs). ESMs combine ocean, atmosphere, land, and sea-ice models to investigate feedbacks in energy and carbon flows within the Earth system. These are the models that are used for future climate predictions, for example, for the International Panel on Climate Change (IPCC) assessments. In association with each IPCC report, the biogeochemical modeling community conducts intercomparisons (Carbon Model Intercomparison Project). The CMIP6 model assessment was used for the IPCC Sixth Assessment. One of the major advances between CMIP5 and CMIP6 was the increased complexity of organic matter cycling and how it is represented in these models (Séférian et al., 2020).

All ESMs represent at least one organic matter pool, and many have multiple DOM pools (Séférian et al., 2020). Typically these DOM pools are operationally defined based on the turn-over timescales, with the SLDOM pool turning over on seasonal to annual timescales, the SRDOM pool turning over on multiannual to decadal timescales, and the RDOM pool turning over on millennial timescales (e.g., Long et al., 2021; Stock et al., 2020; Aumont et al., 2015). These models typically represent the production of DOM driven by phytoplankton

exudation, mortality of phytoplankton and zooplankton, and "sloppy feeding" by zooplankton on phytoplankton, as described before (Eq. 18.4). In most ESMs, the consumption of DOM is represented as a loss rate which is sometimes temperature dependent (e.g., Stock et al., 2020), light dependent (e.g., Long et al., 2021), and/or oxygen dependent (e.g., Aumont et al., 2015). In these models, heterotrophic bacteria are typically implicit, and their metabolism of OM is represented by a single rate constant. A few ESMs explicitly represent a bacterial group that consumes LDOM (e.g., Stock et al., 2020). As all of these models couple biology, chemistry, and physics, they also capture DOM export out of the surface ocean due to mixing and subduction, which has been shown to be an important loss process for DOM in the surface ocean (Resplandy et al., 2019; Copin-Montégut and Avril, 1993; Carlson et al., 1994; Hansell and Carlson, 2001; Dall'Olmo et al., 2016; Boyd et al., 2019; Le Moigne, 2019). Of note, most of these models do not represent RDOM that cycles on millennial time-scales. As a result, these models struggle to capture observed DOM pools (see following sections for further discussion).

Some widely used biogeochemical models include PISCES-v2 (Aumont et al., 2015) that is implemented in several Earth System Models, including the IPSL and CNRM models, and represents one pool of SLDOM; the COBALT-v2 model that is implemented in the GFDL Earth System Model, and represents three DOM pools (LDOM, SLDOM, RDOM) (Stock et al., 2020); and the MARBL-BEC model that is implemented in the Community Earth System Model and represents SLDOM and RDOM pools (Long et al., 2021). A review of these models can be found in Séférian et al. (2020).

18.3 Modeling more complex organic matter dynamics

Models of organic matter cycling represent only a small fraction of the existing chemical diversity in the DOM pool. Simplifying DOM into bulk pools based on differences in turnover rates (e.g., SLDOM, RDOM) provides a good first-order approximation when considering energy and carbon flows through an ecosystem. Specifically, incorporating these broad DOM classes into biogeochemical and ecosystem models allows these models to better capture observed turnover rates for nutrient pools and the timing and magnitude of phytoplankton population shifts (see Section 18.2.1). However, this simplification does not allow for varying microbial DOM consumers to impact rates of DOM cycling. The representation of DOM in most numerical biogeochemical models assumes that the turnover rate of the organic matter compounds is inherent to the compound and independent of the microbial community. Both modeling (Zakem et al., 2021; Nguyen et al., 2022) and experimental work (e.g., Carlson et al., 2004; Liu et al., 2020) have demonstrated that this is not always true. Specifically, turnover rates for DOM can be ecosystem dependent such that the biological-chemical interactions become important for determining degradation rates. These dynamics are not incorporated into most models of OM cycling (DOM and POM) in part due to a limited understanding of the underlying mechanisms driving these processes.

While the impact of a diverse OM pool has not been included in most models of OM cycling, significant progress has been made on modeling differential rates of DON, DOP, and DOC cycling. In practice, this means breaking up Eq. (18.4) to represent multiple types

of DOM and separately track DOC, DON, and DOP. These studies have shown that variable organic matter stoichiometry can substantially impact biogeochemical cycling and ecosystem processes.

Letscher et al. (Letscher and Moore, 2015; Letscher et al., 2015) incorporated variable DOM stoichiometry into a biogeochemical model. Like previous models, DOM is produced as a fraction of primary productivity. However, the turnover rates of the DOM pool differ such that DOP is turned over more quickly than DOC, due to the preferential consumption of phosphorous-containing compounds by marine microbes. The differential cycling of DOC and DOP resulted in a modest but significant impact on primary productivity (8% increase globally) and carbon export (9% increase), with the majority of this increase due to DOP uptake by phytoplankton. These dynamics had the largest impact on nitrogen fixation, increasing rates by 25%. Lateral transport of surplus DON and DOP from more productive regions toward the oligotrophic ocean was shown to be an important process for retaining nutrients in the upper ocean that would otherwise be exported vertically, helping to supply a significant fraction of subtropical gyre nutrient budgets (Letscher et al., 2016).

Many models of OM cycling use a black-box representation of microbial dynamics in which details of microbial processes are lacking. Work by Zakem and Levine (2019) used a model to suggest mechanisms behind the preferential remineralization of DOP and DON observed by Letscher (Letscher and Moore, 2015; Letscher et al., 2015) and parameterized in some ESMs (e.g., Long et al., 2021). Using a quota model to investigate preferential uptake patterns by heterotrophic bacteria, Zakem and Levine (2019) were able to capture observed patterns of DOC and DON with depth. This modeling work suggested that shifts in the stoichiometry of DOM produced by phytoplankton can have large effects on the recycling of nutrients in the surface ocean and, thus, rates of primary production and carbon export. Specifically, because LDOM does not show preferential remineralization, the relative amounts of recalcitrant DOM production versus LDOM production impacts not only carbon cycling but also nitrogen and phosphorus cycling.

DOM cycling is also important for iron cycling and ecosystem dynamics (*see Chapter 10 for further discussion about metal binding ligands*). In many regions of the ocean, iron limits primary productivity, and organic ligands play a key role in regulating the bioavailability of iron. However, most biogeochemical models do not represent this process. Biogeochemical models that incorporate iron-binding ligands have shown that the distribution of bioavailable iron is significantly impacted by how iron-binding ligands are represented in the model and that this has important implications for primary productivity (e.g., Tagliabue et al., 2016; Völker and Tagliabue, 2015). These models typically explicitly incorporate iron-binding ligands by linking ligand production to the DOM pool.

18.4 Data-constrained models of DOC cycling

Most of the mechanistic biogeochemical models implemented in ESMs and described in Section 18.2 represent the cycling of short-lived LDOM to SLDOM (Fig. 18.1B). While these shorter-lived DOM pools play an important role in ecosystem dynamics and nutrient cycling, they represent only a fraction of the total DOM inventory, most of which turns over on much longer timescales (Hansell, 2013). It is challenging for biogeochemical models to resolve the

long-lived RDOM pools because lengthy simulations are required to "spin-up" the model so that the DOM cycle comes to equilibrium—this timescale is at least 10,000 years for the most refractory pools. These factors and biases in the deep ocean overturning of these models can lead to errors in their simulated DOM distribution (e.g., Long et al., 2021). Thus a different class of model is needed to assess the global distributions and cycling of the entire DOM pool.

Several approaches have been developed to address the challenge of accurately simulating the global distribution of DOM, with a focus on DOC. All of the models described in this section give a global view of DOC concentrations and production rates that are consistent with (and constrained by) DOC observations. Given the sparsity of oceanographic measurements, these models provide a means for gap-filling sparse data and generating global-scale assessments of DOC concentrations and inventories. Furthermore, the models can assess biogeochemical rates and turnover times that are not apparent from observations of standing stocks alone.

One modeling approach uses transport matrix (TM) models that represent ocean circulation and mixing as a sparse matrix transport operator (e.g., Primeau, 2005; Khatiwala et al., 2005). The TM can be used as the circulation component of ocean biogeochemical models (see Eqs. 18.1–18.4). The advantage of TM-based models is that they are amenable to fast spin-up methods, greatly reducing the simulation times necessary to achieve an equilibrium DOM cycle. One of the earliest TM-based models of DOC cycling is that of Hansell et al. (2009, 2012). Their studies consist of a simple DOC cycling model embedded in the data-constrained circulation model of Schlitzer (2007). The model represents three different DOC pools—SLDOC, SRDOC, and RDOC—with lifetimes of 1.5–3 years, 10–20 years, and 15,000–16,000 years, respectively (exact lifetimes depending on the model configuration). DOC production in the euphotic zone is proportional to the square root of the satellite-derived primary production (PP), and the production rates of each fraction are adjusted to achieve the best match to DOC observations. Hereafter we will refer to this as the DOC TM model.

Another TM-based model is the data-constrained ocean biogeochemical model of DeVries and Weber (2017). This biogeochemical model is coupled to a TM from an ocean circulation inverse model (OCIM) (DeVries, 2014). The OCIM is a data-assimilated model whose circulation is optimized to match the distribution of physical tracers such as temperature, salinity, and CFCs. The biogeochemical model represents four DOC pools (labile, semilabile, semirefractory, refractory) with lifetimes of ~10 days, ~2 years, ~200 years, and ~50,000 years, respectively. DOC in this model is produced in the euphotic zone as a fraction of satellite-derived PP rates. The rate of DOC production varies by plankton type (large or small), as does the fraction of DOC production allocated to different DOC pools. These parameters, as well as degradation rates for the four DOC pools, are adjusted to match DOC observations. A later update to this model by Nowicki et al. (2022) added an explicit ecosystem model and updated the parameters to maintain a good match to observed DOC. Hereafter we will refer to these models (either version) as the biogeochemical TM model.

An alternative approach utilized by Roshan and DeVries (2017) modeled total DOC concentrations using an Artificial Neural Network (ANN). The ANN model predicts the total DOC concentration in the ocean using climatologies of nutrients, temperature, salinity, and other oceanographic observations as inputs. Roshan and DeVries (2017) used the ANN-predicted DOC concentrations to estimate net DOC production and export rates. They did this by using the OCIM to calculate the circulation-induced transport of DOC in Eq. (18.4),

and then estimating the net production (production—loss, i.e. the right-hand side of Eq. 18.4) of DOC in the euphotic zone by restoring the modeled DOC to the ANN-predicted DOC concentrations (Roshan and DeVries, 2017). Hereafter we will refer to this model, including the diagnosed net source of DOC, as the ANN model.

In Sections 18.5 and 18.6, we discuss results of these data-constrained models with a focus on the global cycling and budgets of DOC. Other components of DOM such as DON and DOP have only recently been simulated with these types of models (e.g., Letscher et al., 2022), and their budgets are not discussed here.

18.5 Global distribution, inventories, and production rates of DOC

The distributions of DOC predicted by the three different data-constrained models described in Section 18.4 are shown in Fig. 18.2 for the surface ocean (roughly the upper 30 m) and the deep ocean at 2000 m. The models all predict that DOC concentrations are highest in the surface ocean, with concentrations reaching up to $70-80 \,\mu\text{mol}\,\text{kg}^{-1}$ in the tropical and subtropical oceans. In the polar and subpolar surface oceans, DOC concentrations are generally less than 50 µmol kg⁻¹. In the DOC TM and biogeochemical TM models, the high DOC concentrations in the tropical and subtropical surface waters are caused by the production and buildup of SLDOC in these regions. The ANN model does not simulate the mechanisms responsible for the geographic variations of DOC, but exhibits similar patterns to the TM models with high DOC concentrations in the tropics and subtropics, and lowest DOC concentrations in the subpolar North Pacific and Southern Ocean, consistent with large-scale patterns seen in the surface observations (Hansell et al., 2009; Letscher et al., 2015). Beyond these broad similarities, there are some differences in the surface DOC distributions simulated by these data-constrained models. The biogeochemical TM model has larger DOC concentrations near the coasts and slightly lower concentrations in the tropical Pacific than the DOC TM model, while the ANN model has higher DOC concentrations in the western tropical Pacific than either of the other models.

In the deep ocean, DOC is dominated by the refractory component, with a small contribution from SRDOC. Both the DOC TM model and the biogeochemical TM model display a gradual decrease in DOC from the North Atlantic to the North Pacific (Fig. 18.2), consistent with the slow removal of RDOC as water masses age along the deep-ocean conveyor circulation (Carlson et al., 2010; Hansell and Carlson, 1998; Hansell et al., 2009). This deep-ocean turnover is the sole means of refractory DOC removal in these models. The ANN model shows more small-scale structure and variability in the deep-ocean DOC concentration, with more DOC in the Indian Ocean and the western Pacific than is found in the DOC TM and biogeochemical TM models (Fig. 18.2). This is consistent with localized sources and sinks of refractory DOC in the deep ocean, which have been shown to be associated with hydrothermal vents and crustal aquifers (Hawkes et al., 2015; McCarthy et al., 2011; Shah Walter et al., 2018) or marine sediments (Hwang et al., 2010; Pohlman et al., 2011). These localized deep-ocean sources and sinks of DOC are not represented in the DOC or biogeochemical TM models.

The global inventory of DOC ranges from 647GtC in the biogeochemical TM model of Nowicki et al. (2022) to 670GtC in the ANN model of Roshan and DeVries (2017) (Table 18.1). The vast majority of this DOC is in the refractory pool, which comprises

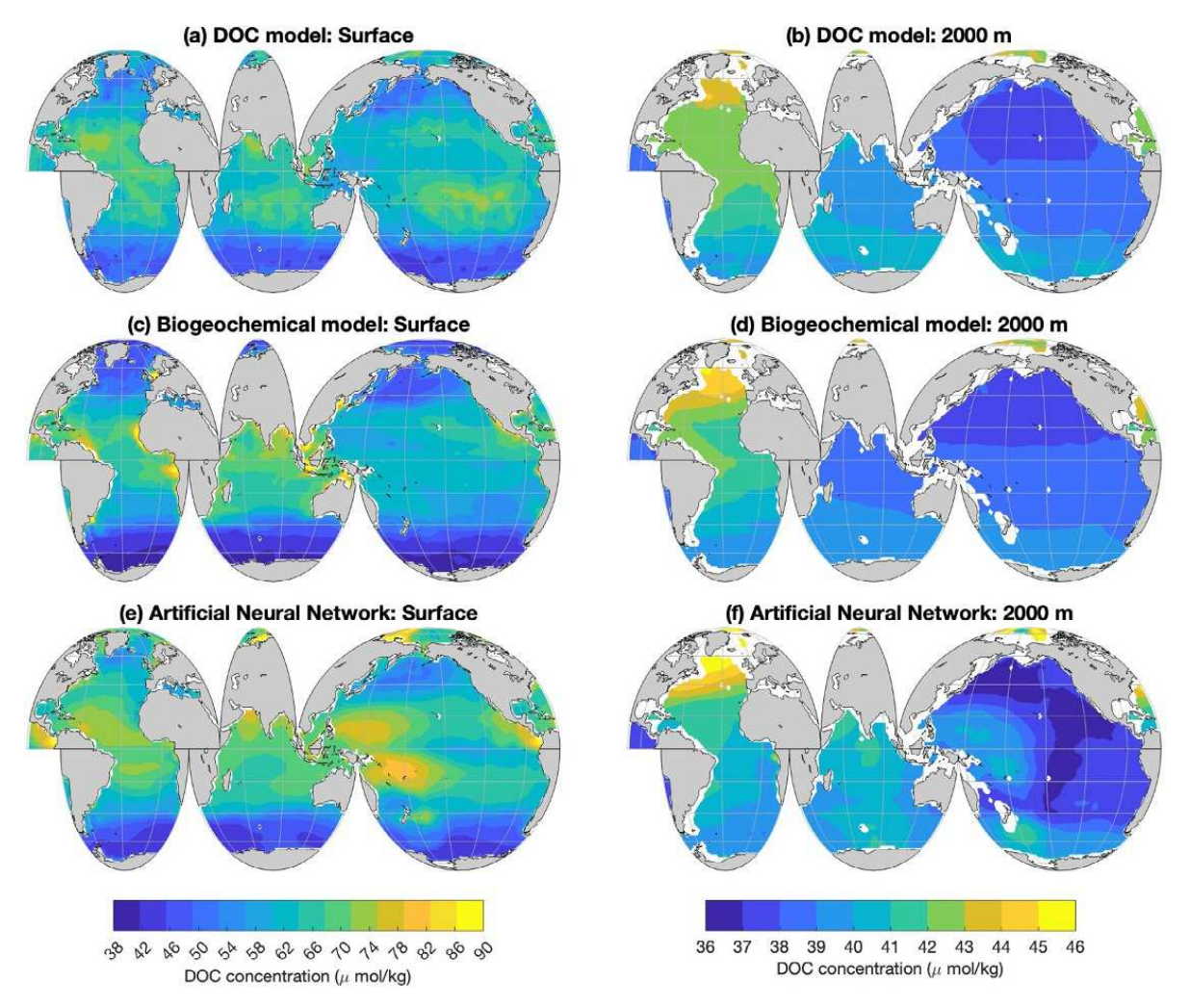


FIG. 18.2 Surface (upper 30 m) and deep-ocean (~2000 m) concentrations of DOC from (A–B) the DOC TM model (Hansell et al., 2009), (C–D) the biogeochemical TM model (DeVries and Weber, 2017), and (E–F) the Artificial Neural Network (ANN) model (Roshan and DeVries, 2017).

 $628-642\,\mathrm{GtC}$ in the models considered here (Table 18.1). Production rates of RDOC range from $0.011\,\mathrm{to}\,0.054\,\mathrm{GtC}\,\mathrm{year}^{-1}$, for a mean lifetime of $\sim 12,000-57,000\,\mathrm{years}$. SRDOC is the next most prominent pool in these models, with an inventory of $9-26\,\mathrm{GtC}$, a production rate of $0.13-0.34\,\mathrm{GtC}\,\mathrm{year}^{-1}$, and a mean lifetime of $30-200\,\mathrm{years}$. It is probable that the wide range of lifetimes and production rates obtained for the SRDOC and RDOC results from the models approximating a continuum of DOC reactivities (Amon and Benner, 1996) within discrete pools. SLDOC is the smallest pool of DOC that accumulates to measurable concentrations in the ocean and amounts to $6-7\,\mathrm{GtC}$ globally, with a global production rate of $3.4-4.6\,\mathrm{GtC}\,\mathrm{year}^{-1}$. Semilabile DOC's inventory and production rate is fairly similar across all these data-constrained models, leading to a fairly well-constrained lifetime of $\sim 1.5-2\,\mathrm{years}$.

TABLE 18.1 Ocean DOC inventory and production rates.

Model	Semilabile DOC	Semirefractory DOC	Refractory DOC	Total DOC
Hansell et al. (2012)	6 3.4	14 0.34	642 0.043	662
DeVries and Weber (2017)	7 3.8	26 0.13	628 0.011	662
Roshan and DeVries (2017)	_	-	_	670
Nowicki et al. (2022)	7 4.6	9 0.30	630 0.054	647

Inventories in bold (GtC) and production rates in italics (GtC year $^{-1}$).

18.6 Carbon export and sequestration by DOC

The formation of long-lived DOC fractions mediated by the microbial carbon pump (Jiao et al., 2010) results in 628–642GtC that is sequestered as RDOC with an extremely long (>10,000 year) turnover time (Table 18.1). The shorter-lived fractions of DOC have global inventories of <~30GtC (Table 18.1), but they can still contribute to carbon sequestration through their role in the biological carbon pump, specifically the so-called mixing pump (Resplandy et al., 2019; Boyd et al., 2019; Le Moigne, 2019). The role of DOC in the biological pump is mitigated predominantly by SLDOC, which is formed in the surface ocean, and exported to the deeper layers by seasonal deepening and shoaling of the mixed layer (Hansell and Carlson, 2001; Dall'Olmo et al., 2016; Carlson et al., 1994), by eddy subduction (Omand et al., 2015), and by the large-scale overturning and subduction of water masses (Carlson et al., 2010; Hansell et al., 2009). Once transported to depth, SLDOC is remineralized back to DIC, contributing to the sequestration of biogenic DIC in the deep ocean (Siegel et al., 2023).

The data-constrained models considered here estimate a DOC export of around 1.6–2.3GtCyear⁻¹, which depends somewhat on the depth horizon at which DOC export is calculated (Table 18.2). This is $\sim 15\%$ –20% of the approximately 10–12 Gt Cyear⁻¹ total export by the biological carbon pump (Hansell et al., 2009). The geographic distribution of carbon export from the biogeochemical TM model (DeVries and Weber, 2017) is illustrated in Fig. 18.3. DOC export is concentrated in three main regions: the northern subtropics, the southern subtropics, and the Southern Ocean north of the polar frontal region. The subtropics are regions in which DOC is subducted in the wind-driven subtropical gyre circulation. A substantial portion of the DOC that is exported in the subtropical gyres originates from DOC produced in the tropical oceans and advected into the subtropical gyres by equatorial current systems (Nowicki et al., 2022; Roshan and DeVries, 2017). The proportion of total carbon export due to DOC varies significantly by latitude (Fig. 18.3). It is lowest along the equator, where diverging surface currents transport DOC to higher latitudes before being exported. It is highest in the subtropical gyres and the sub-Antarctic region where DOC is exported with subducting water masses. The biogeochemical TM model of DeVries and Weber suggests that DOC export is \sim 20%–25% of the total export in subtropical latitudes

TABLE 18.2 DOC export and sequestration by the biological carbon pump.

Model	DOC export (GtCyear ⁻¹)	Sequestration of biogenic DIC (GtC)	Sequestration time (year)
Hansell et al. (2009)	1.8 ^a	_	_
DeVries and Weber (2017)	1.6 ^b	81	51
Roshan and DeVries (2017)	$2.3 \pm 0.6^{\circ}$	_	_
Nowicki et al. (2022)	1.9 ± 0.3^{b}	102	54

^a At 100 m.

^c At 75 m.

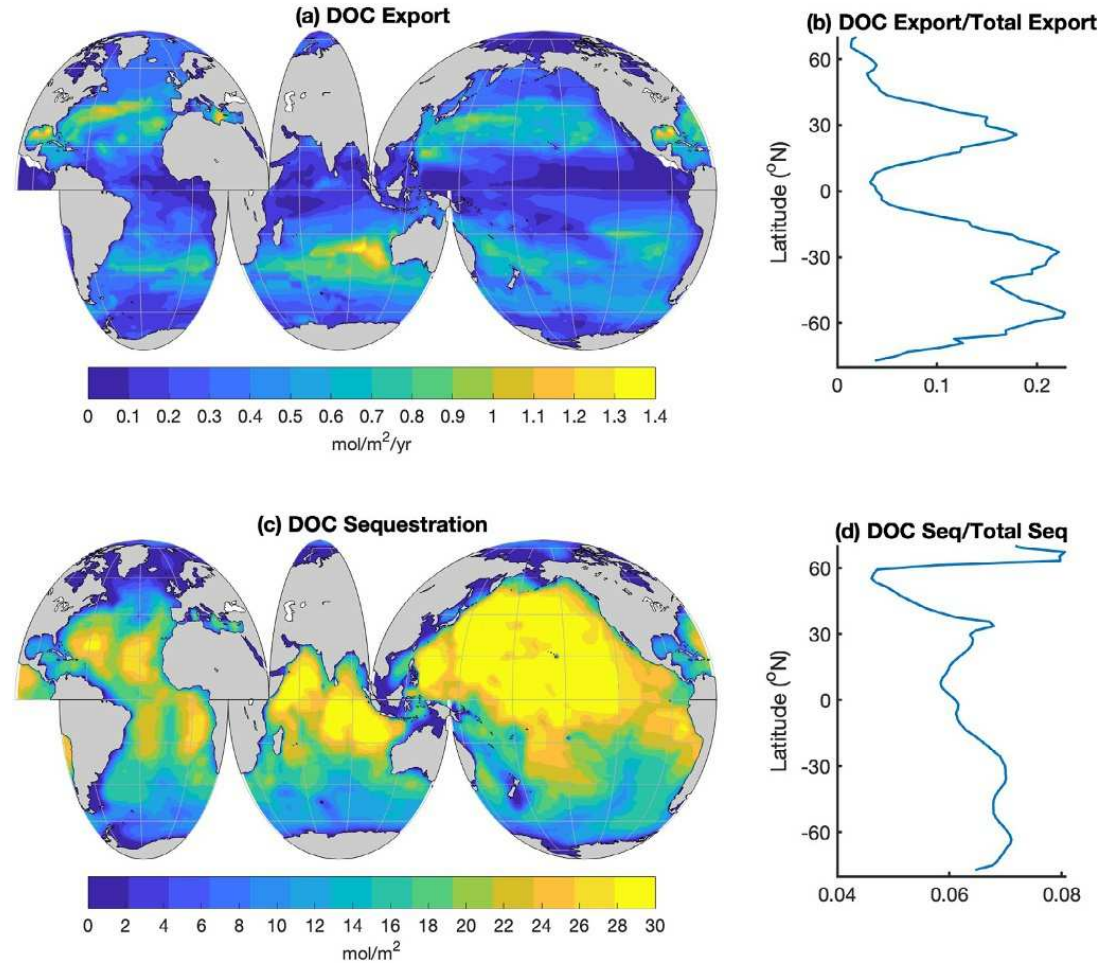


FIG. 18.3 (A) DOC export at the base of the euphotic zone, (B) the ratio of DOC export to total export as a function of latitude, (C) the total amount of biogenic DIC sequestration due to DOC export and remineralization, and (D) the ratio of the DOC-driven DIC sequestration to total biogenic DIC sequestration. All results are from the biogeochemical TM model (DeVries and Weber, 2017).

 $^{^{}b}$ At base of euphotic zone.

(Fig. 18.3), while the ANN-derived diagnostic model of Roshan and DeVries (2017) predicts that the proportion of DOC to particulate organic carbon (POC) export in the subtropical gyres can reach up to 70%.

The models considered here (Fig. 18.3 and Table 18.2) resolve only the large-scale ocean circulation, and do not resolve small-scale processes such as eddy subduction, which has been hypothesized to export large amounts of suspended and dissolved organic carbon. These small-scale processes might increase the proportion of DOC export in the ocean above these model predictions (Resplandy et al., 2019).

Once DOC is exported and remineralized in the interior ocean, the resulting biogenic DIC contributes to carbon sequestration by the biological carbon pump (Boyd et al., 2019; Nowicki et al., 2022). The biogeochemical TM models (DeVries and Weber, 2017; Nowicki et al., 2022) estimate that DOC sequesters around 80–100GtC in the interior ocean as biogenic DIC (Table 18.2) or ~6%–8% of the total biogenic carbon sequestration of roughly 1300GtC (Nowicki et al., 2022; Carter et al., 2021). The sequestration time for biogenic DIC derived from DOC export is around 50 years, representing the mean time that biogenic DIC derived from exported SLDOC is sequestered in the interior ocean before being reexposed at the sea surface. By contributing to biogenic carbon sequestration, SLDOC exerts a climatic control that is greater than its relatively small inventory would suggest.

18.7 Areas for future advancement in DOM modeling

The current state-of-the-art biogeochemical models can capture carbon and energy flows through marine ecosystems and standing stocks of DOM, while data-constrained models have been able to illuminate the global cycling and budgets of DOC. Despite these advances, there are several key areas where further model development is necessary.

Mechanistic biogeochemical models have primarily focused on carbon and energy fluxes. Thus these models typically do not represent the RDOC pool which turns over on millennial timescales, as it is not believed to play a significant role in short-term ecosystem dynamics. However, this refractory pool makes up the bulk of the total DOC and so plays an important role in long-term carbon cycle dynamics. Data-constrained models are able to represent this pool but lack the full ecological and biogeochemical dynamics of mechanistic models. A key future advancement will be incorporating these refractory pools in mechanistic biogeochemical models by using new computational methods to shorten spin-up times (Lindsay, 2017).

While early models used fixed (typically Redfield) stoichiometries for DOM, state-of-the-art models incorporate variable DOM stoichiometries (e.g., Letscher et al., 2015; Letscher and Moore, 2015). These studies have demonstrated the importance of this biologically driven variability for determining primary production and carbon export. Developing models that make the link between variable phytoplankton and zooplankton stoichiometries and that of the DOM pools will help to advance our understanding of nutrient cycling in the ocean and the role that DOM plays in global biogeochemical cycles.

Nearly all DOM models represent only a handful of OM pools, while in reality, we know that DOM is incredibly complex and composed of thousands of different compounds. Some models focused specifically on the complexity of DOM have included thousands of DOM pools (e.g., Zakem et al., 2021; Mentges et al., 2019) (see Chapter 13 for a detailed discussion of

References 817

these models). These models have shown that representing the complex dynamics of diverse DOM compounds can provide insight into DOM standing stocks and mechanistic insight into variable rates of DOM turnover. Reconciling these two different extremes (a few vs thousands) of DOM pools to allow models to capture the first-order dynamics associated with DOM cycling is an important challenge that needs to be overcome.

Incorporating more realistic DOM cycling within models will also rely on an improved understanding of both production and loss mechanisms. Specifically, DOM production in models is currently vaguely defined and linked (typically linearly) to rates of primary production and mortality. More work is needed to understand how DOM production rates vary as a function of different release mechanisms, for example, "sloppy feeding" versus viral lysis versus exudation. Similarly, experimental work is needed to understand how variations in heterotrophic microbial community compositions impact rates of DOM cycling and how the chemical structure of DOM changes through this process. DOM models then have the potential to provide critical insight by integrating new biological knowledge of these processes with the new chemical understanding of chemical complexity and rates of transformation and/or degradation.

Finally, the majority of large-scale DOM models focus on marine sources and sinks of DOM, with most production occurring through ecosystem processes in the euphotic zone and most removal due to bacterial consumption throughout the water column (*see discussion in Section 18.2*). However, the cycling of DOM is considerably more complex with multiple external sources and sinks of DOM to the ocean (*as discussed in Chapters 6, 7, and 14*). Specifically, rivers (Medeiros et al., 2016), hydrothermal vent systems (McCarthy et al., 2011), and sediments (Holcombe et al., 2001) all act as DOM sources and are typically missing from large-scale DOM models, aside from riverine sources which are implemented in some models (e.g., Long et al., 2021). External sinks of DOM include photooxidation (Mopper et al., 1991) (*see Chapter 11*), marine aerosols (Kieber et al., 2016), and hydrothermal circulation (Hawkes et al., 2016). These external sources and sinks may be particularly important for the aged RDOC pools that comprise the vast majority of the DOC inventory. Thus, representing these processes and their dynamics in models should be a priority for future model development.

Acknowledgments

The authors would like to acknowledge the fruitful conversations and collaborations with many colleagues over the years that have contributed to this chapter. In particular, Craig Carlson, Dennis Hansell, Emily Zakem, Rob Letscher, Ferdi Hellweger, Reiner Schlitzer, Michael Nowicki, and Saeed Roshan. We would also like to thank the NSF Chemical Oceanography program in particular support for TD through grant OCE-2049509, NSF Biological Oceanography program, and the Simons Foundation for their support of NML through grant 542389.

References

Amon, R.M., Benner, R., 1996. Bacterial utilization of different size classes of dissolved organic matter. Limnol. Oceanogr. 41 (1), 41–51.

Aumont, O., Éthé, C., Tagliabue, A., Bopp, L., Gehlen, M., 2015. PISCES-v2: an ocean biogeochemical model for carbon and ecosystem studies. Geosci. Model Dev. Discuss. 8 (2), 1375–1509.

Benner, R., Amon, R.M., 2015. The size-reactivity continuum of major bioelements in the ocean. Annu. Rev. Mar. Sci. 7, 185–205.

- Boyd, P.W., Claustre, H., Levy, M., Siegel, D.A., Weber, T., 2019. Multi-faceted particle pumps drive carbon sequestration in the ocean. Nature 568 (7752), 327–335.
- Carlson, C.A., Ducklow, H.W., Michaels, A.F., 1994. Annual flux of dissolved organic carbon from the euphotic zone in the northwestern Sargasso Sea. Nature 371 (6496), 405–408.
- Carlson, C.A., Giovannoni, S.J., Hansell, D.A., Goldberg, S.J., Parsons, R., Vergin, K., 2004. Interactions among dissolved organic carbon, microbial processes, and community structure in the mesopelagic zone of the north-western Sargasso Sea. Limnol. Oceanogr. 49 (4), 1073–1083.
- Carlson, C.A., Hansell, D.A., Nelson, N.B., Siegel, D.A., Smethie, W.M., Khatiwala, S., Meyers, M.M., Halewood, E., 2010. Dissolved organic carbon export and subsequent remineralization in the mesopelagic and bathypelagic realms of the North Atlantic basin. Deep-Sea Res. II Top. Stud. Oceanogr. 57 (16), 1433–1445.
- Carter, B.R., Feely, R.A., Lauvset, S.K., Olsen, A., DeVries, T., Sonnerup, R., 2021. Preformed properties for marine organic matter and carbonate mineral cycling quantification. Glob. Biogeochem. Cycles 35 (1), e2020GB006623.
- Copin-Montégut, G., Avril, B., 1993. Vertical distribution and temporal variation of dissolved organic carbon in the North-Western Mediterranean Sea. Deep-Sea Res. I Oceanogr. Res. Pap. 40 (10), 1963–1972.
- Dall'Olmo, G., Dingle, J., Polimene, L., Brewin, R.J., Claustre, H., 2016. Substantial energy input to the mesopelagic ecosystem from the seasonal mixed-layer pump. Nat. Geosci. 9 (11), 820–823.
- DeVries, T., 2014. The oceanic anthropogenic CO₂ sink: storage, air-sea fluxes, and transports over the industrial era. Glob. Biogeochem. Cycles 28 (7), 631–647.
- DeVries, T., Weber, T., 2017. The export and fate of organic matter in the ocean: new constraints from combining satellite and oceanographic tracer observations. Glob. Biogeochem. Cycles 31 (3), 535–555.
- Doney, S.C., Glover, D.M., Najjar, R.G., 1996. A new coupled, one-dimensional biological-physical model for the upper ocean: applications to the JGOFS Bermuda Atlantic time-series study (BATS) site. Deep-Sea Res. II Top. Stud. Oceanogr. 43 (2-3), 591–624.
- Fasham, M.J.R., Ducklow, H.W., McKelvie, S.M., 1990. A nitrogen-based model of plankton dynamics in the oceanic mixed layer. J. Mar. Res. 48 (3), 591–639.
- Hansell, D.A., 2013. Recalcitrant dissolved organic carbon fractions. Mar. Sci. 5.
- Hansell, D.A., Carlson, C.A., 1998. Net community production of dissolved organic carbon. Glob. Biogeochem. Cycles 12 (3), 443–453.
- Hansell, D.A., Carlson, C.A., 2001. Biogeochemistry of total organic carbon and nitrogen in the Sargasso Sea: control by convective overturn. Deep-Sea Res. II Top. Stud. Oceanogr. 48 (8-9), 1649–1667.
- Hansell, D.A., Carlson, C.A., Repeta, D.J., Schlitzer, R., 2009. Dissolved organic matter in the ocean: a controversy stimulates new insights. Oceanography 22 (4), 202–211.
- Hansell, D.A., Carlson, C.A., Schlitzer, R., 2012. Net removal of major marine dissolved organic carbon fractions in the subsurface ocean. Glob. Biogeochem. Cycles 26 (1).
- Hawkes, J.A., Rossel, P.E., Stubbins, A., Butterfield, D., Connelly, D.P., Achterberg, E.P., Koschinsky, A., Chavagnac, V., Hansen, C.T., Bach, W., 2015. Efficient removal of recalcitrant deep-ocean dissolved organic matter during hydrothermal circulation. Nat. Geosci. 8 (11), 856–860.
- Hawkes, J.A., Hansen, C.T., Goldhammer, T., Bach, W., Dittmar, T., 2016. Molecular alteration of marine dissolved organic matter under experimental hydrothermal conditions. Geochim. Cosmochim. Acta 175, 68–85.
- Holcombe, B.L., Keil, R.G., Devol, A.H., 2001. Determination of pore-water dissolved organic carbon fluxes from Mexican margin sediments. Limnol. Oceanogr. 46 (2), 298–308.
- Hwang, J., Druffel, E.R., Eglinton, T.I., 2010. Widespread influence of resuspended sediments on oceanic particulate organic carbon: Insights from radiocarbon and aluminum contents in sinking particles. Glob. Biogeochem. Cycles 24 (4).
- Jamart, B.M., Winter, D., Banse, K., Anderson, G., Lam, R., 1977. A theoretical study of phytoplankton growth and nutrient distribution in the Pacific Ocean off the northwestern US coast. Deep-Sea Res. 24 (8), 753–773.
- Jiao, N., Herndl, G.J., Hansell, D.A., Benner, R., Kattner, G., Wilhelm, S.W., Kirchman, D.L., Weinbauer, M.G., Luo, T., Chen, F., 2010. Microbial production of recalcitrant dissolved organic matter: long-term carbon storage in the global ocean. Nat. Rev. Microbiol. 8 (8), 593–599.
- Khatiwala, S., Visbeck, M., Cane, M.A., 2005. Accelerated simulation of passive tracers in ocean circulation models. Ocean Model. 9 (1), 51–69.
- Kieber, D.J., Keene, W.C., Frossard, A.A., Long, M.S., Maben, J.R., Russell, L.M., Kinsey, J.D., Tyssebotn, I.M.B., Quinn, P.K., Bates, T.S., 2016. Coupled ocean-atmosphere loss of marine refractory dissolved organic carbon. Geophys. Res. Lett. 43 (6), 2765–2772.

References 819

- Kiefer, D.A., Kremer, J.N., 1981. Origins of vertical patterns of phytoplankton and nutrients in the temperate, open ocean: a stratigraphic hypothesis. Deep Sea Res. A Oceanogr. Res. Pap. 28 (10), 1087–1105.
- Le Moigne, F.A., 2019. Pathways of organic carbon downward transport by the oceanic biological carbon pump. Front. Mar. Sci. 6, 634.
- Letscher, R.T., Moore, J.K., 2015. Preferential remineralization of dissolved organic phosphorus and non-Redfield DOM dynamics in the global ocean: Impacts on marine productivity, nitrogen fixation, and carbon export. Glob. Biogeochem. Cycles 29 (3), 325–340.
- Letscher, R.T., Moore, J.K., Teng, Y.-C., Primeau, F., 2015. Variable C: N: P stoichiometry of dissolved organic matter cycling in the Community Earth System Model. Biogeosciences 12 (1), 209–221.
- Letscher, R.T., Primeau, F., Moore, J.K., 2016. Nutrient budgets in the subtropical ocean gyres dominated by lateral transport. Nat. Geosci. 9 (11), 815–819.
- Letscher, R.T., Wang, W.L., Liang, Z., Knapp, A.N., 2022. Regionally variable contribution of dissolved organic phosphorus to marine annual net community production. Glob. Biogeochem. Cycles 36 (12), e2022GB007354.
- Lindsay, K., 2017. A Newton-Krylov solver for fast spin-up of online ocean tracers. Ocean Model. 109, 33-43.
- Liu, S., Parsons, R., Opalk, K., Baetge, N., Giovannoni, S., Bolaños, L.M., Kujawinski, E.B., Longnecker, K., Lu, Y., Halewood, E., 2020. Different carboxyl-rich alicyclic molecules proxy compounds select distinct bacterioplankton for oxidation of dissolved organic matter in the mesopelagic Sargasso Sea. Limnol. Oceanogr. 65 (7), 1532–1553.
- Long, M.C., Moore, J.K., Lindsay, K., Levy, M., Doney, S.C., Luo, J.Y., Krumhardt, K.M., Letscher, R.T., Grover, M., Sylvester, Z.T., 2021. Simulations with the marine biogeochemistry library (MARBL). J. Adv. Model. Earth Syst. 13 (12), e2021MS002647.
- McCarthy, M.D., Beaupré, S.R., Walker, B.D., Voparil, I., Guilderson, T.P., Druffel, E.R., 2011. Chemosynthetic origin of 14C-depleted dissolved organic matter in a ridge-flank hydrothermal system. Nat. Geosci. 4 (1), 32–36.
- Medeiros, P.M., Seidel, M., Niggemann, J., Spencer, R.G., Hernes, P.J., Yager, P.L., Miller, W.L., Dittmar, T., Hansell, D.A., 2016. A novel molecular approach for tracing terrigenous dissolved organic matter into the deep ocean. Glob. Biogeochem. Cycles 30 (5), 689–699.
- Mentges, A., Feenders, C., Deutsch, C., Blasius, B., Dittmar, T., 2019. Long-term stability of marine dissolved organic carbon emerges from a neutral network of compounds and microbes. Sci. Rep. 9 (1), 1–13.
- Moore, J.K., Doney, S.C., Kleypas, J.A., Glover, D.M., Fung, I.Y., 2002. An intermediate complexity marine ecosystem model for the global domain. Deep-Sea Res. II Top. Stud. Oceanogr. 49 (1-3), 403–462.
- Mopper, K., Zhou, X., Kieber, R.J., Kieber, D.J., Sikorski, R.J., Jones, R.D., 1991. Photochemical degradation of dissolved organic carbon and its impact on the oceanic carbon cycle. Nature 353 (6339), 60–62.
- Najjar, R.G., Sarmiento, J.L., Toggweiler, J., 1992. Downward transport and fate of organic matter in the ocean: simulations with a general circulation model. Glob. Biogeochem. Cycles 6 (1), 45–76.
- Nguyen, T.T., Zakem, E.J., Ebrahimi, A., Schwartzman, J., Caglar, T., Amarnath, K., Alcolombri, U., Peaudecerf, F.J., Hwa, T., Stocker, R., Cordero, O.X., Levine, N.M., 2022. Microbes contribute to setting the ocean carbon flux by altering the fate of sinking particulates. Nat. Commun. 13 (1), 1657.
- Nowicki, M., DeVries, T., Siegel, D.A., 2022. Quantifying the carbon export and sequestration pathways of the ocean's biological carbon pump. Glob. Biogeochem. Cycles 36 (3), e2021GB007083.
- Omand, M.M., D'Asaro, E.A., Lee, C.M., Perry, M.J., Briggs, N., Cetinic, I., Mahadevan, A., 2015. Eddy-driven subduction exports particulate organic carbon from the spring bloom. Science 348 (6231), 222–225.
- Omand, M.M., Govindarajan, R., He, J., Mahadevan, A., 2020. Sinking flux of particulate organic matter in the oceans: sensitivity to particle characteristics. Sci. Rep. 10 (1), 5582.
- Pace, M., Glasser, J., Pomeroy, L., 1984. A simulation analysis of continental shelf food webs. Mar. Biol. 82, 47–63. Pohlman, J.W., Bauer, J.E., Waite, W.F., Osburn, C.L., Chapman, N.R., 2011. Methane hydrate-bearing seeps as a
- source of aged dissolved organic carbon to the oceans. Nat. Geosci. 4 (1), 37–41. Pomeroy, L.R., 1974. The ocean's food web, a changing paradigm. Bioscience 24 (9), 499–504.
- Primeau, F., 2005. Characterizing transport between the surface mixed layer and the ocean interior with a forward and adjoint global ocean transport model. J. Phys. Oceanogr. 35 (4), 545–564.
- Resplandy, L., Lévy, M., McGillicuddy Jr., D.J., 2019. Effects of eddy-driven subduction on ocean biological carbon pump. Glob. Biogeochem. Cycles 33 (8), 1071–1084.
- Riley, G.A., 1946. Factors controlling phytoplankton populations on Georges Bank. J. Mar. Res. 6, 54–71.
- Riley, G.A., 1947. A theoretical analysis of the zooplankton population on Georges Bank. J. Mar. Res. 6 (2), 104–113.
- Riley, G.A., Bumpus, D.F., 1946. Phytoplankton-zooplankton relationships on Georges Bank. J. Mar. Res. 6 (1), 33–47.

- Roshan, S., DeVries, T., 2017. Efficient dissolved organic carbon production and export in the oligotrophic ocean. Nat. Commun. 8 (1), 2036.
- Schlitzer, R., 2007. Assimilation of radiocarbon and chlorofluorocarbon data to constrain deep and bottom water transports in the world ocean. J. Phys. Oceanogr. 37 (2), 259–276.
- Séférian, R., Berthet, S., Yool, A., Palmieri, J., Bopp, L., Tagliabue, A., Kwiatkowski, L., Aumont, O., Christian, J., Dunne, J., 2020. Tracking improvement in simulated marine biogeochemistry between CMIP5 and CMIP6. Curr. Clim. Chang. Rep. 6 (3), 95–119.
- Shah Walter, S.R., Jaekel, U., Osterholz, H., Fisher, A.T., Huber, J.A., Pearson, A., Dittmar, T., Girguis, P.R., 2018. Microbial decomposition of marine dissolved organic matter in cool oceanic crust. Nat. Geosci. 11 (5), 334–339.
- Siegel, D.A., DeVries, T., Cetinić, I., Bisson, K.M., 2023. Quantifying the ocean's biological pump and its carbon cycle impacts on global scales. Annu. Rev. Mar. Sci. 15, 329–356.
- Stock, C.A., Dunne, J.P., John, J.G., 2014. Global-scale carbon and energy flows through the marine planktonic food web: an analysis with a coupled physical-biological model. Prog. Oceanogr. 120, 1–28.
- Stock, C.A., Dunne, J.P., Fan, S., Ginoux, P., John, J., Krasting, J.P., Laufkötter, C., Paulot, F., Zadeh, N., 2020. Ocean biogeochemistry in GFDL's Earth System Model 4.1 and its response to increasing atmospheric CO₂. J. Adv. Model. Earth Syst. 12 (10), e2019MS002043.
- Tagliabue, A., Aumont, O., DeAth, R., Dunne, J.P., Dutkiewicz, S., Galbraith, E., Misumi, K., Moore, J.K., Ridgwell, A., Sherman, E., 2016. How well do global ocean biogeochemistry models simulate dissolved iron distributions? Glob. Biogeochem. Cycles 30 (2), 149–174.
- Vézina, A.F., Platt, T., 1987. Small-scale variability of new production and particulate fluxes in the ocean. Can. J. Fish. Aquat. Sci. 44 (1), 198–205.
- Völker, C., Tagliabue, A., 2015. Modeling organic iron-binding ligands in a three-dimensional biogeochemical ocean model. Mar. Chem. 173, 67–77.
- Williams, P., 1981. Incorporation of microheterotrophic processes into the classical paradigm of the planktonic food web. Kieler Meeresforsch. Sonderh. 5, 1–28.
- Williams, P., Druffel, E., Williams, P., Druffel, E., 1988. Dissolved organic matter in the ocean: comments on a controversy. Oceanography 1 (1), 14–17.
- Zakem, E.J., Levine, N.M., 2019. Systematic variation in marine dissolved organic matter stoichiometry and remineralization ratios as a function of lability. Glob. Biogeochem. Cycles 33 (11), 1389–1407.
- Zakem, E.J., Cael, B., Levine, N.M., 2021. A unified theory for organic matter accumulation. Proc. Natl. Acad. Sci. 118 (6), e2016896118.